Polyhedron 28 (2009) 2001–2009

Contents lists available at ScienceDirect

Polyhedron

journal homepage: www.elsevier.com/locate/poly

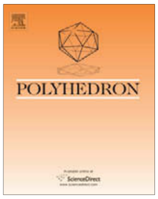

Structures and magnetic properties of imidazolate-bridged tetranuclear and polymeric copper(II) complexes

Nobumasa Koyama, Ryo Watanabe, Takayuki Ishida *, Takashi Nogami, Tamizo Kogane *

Department of Applied Physics and Chemistry, The University of Electro-Communications, Chofugaoka 1-5-1, Chofu, Tokyo 182-8585, Japan

ARTICLE INFO

Article history:
Available online 12 January 2009

Keywords:
Imidazole
Copper(II) ion
Supramolecular chemistry
Magnetic property
Molecular grid

ABSTRACT

Eight kinds of imidazolate-bridged copper(II) complexes were found to be classified into two categories from the magnetic properties. The crystal structures of $[Cu(L)(\mu\text{-im})]_n$ (Him = imidazole; L = nonane-4,6-dionate, 2,6-dimethylheptane-3,5-dionate) and $[Cu(L)(\mu\text{-im})]_4$ (L = nonane-4,6-dionate, 1-phenylbutane-1,3-dionate) were determined, to reveal that they consist of polymeric chains and tetranuclear cycles, respectively. Note that the nonane-4,6-dionate derivative gave the two phases. The Bonner–Fisher model (a one-dimensional antiferromagnetic chain model) was plausibly applied to $[Cu(L)(\mu\text{-im})]_n$ for the best fit, while a square model was to $[Cu(L)(\mu\text{-im})]_4$. The complexes with unknown crystal structures were also subjected to magnetic measurements, and the tetra- and polymeric structures could be clearly distinguished from each other by fitting the magnetic data to appropriate models. The exchange parameters were comparable for both series ($2J/k_B = -78$ to -97 K) because the structurally common bridges Cu–N(eq)–N(eq)–Cu afford comparable magnitudes of couplings.

1. Introduction

Oligonuclear and polymeric copper(II) coordination compounds attract much attention in materials chemistry; for example, Kahn's magnetic material building-blocks [1], Yaghi and co-workers' metal-organic frameworks [2], and Lehn's supramolecular chemistry approach [3]. Some peculiar enzyme functions are based on oligonuclear copper clusters in laccase and ascorbate oxidase [4], where imidazolates and histidinates play a role of bridging ligands. Copper(II) imidazolate systems afford a variety of structures of self-assembled supramolecular coordination complexes, e.g., trinuclear cycles [5], tetranuclear cycles or [2 × 2] grids [6–10], discrete linear systems [11–16], polymeric chains [17,18], layers [19–21], and 3-D networks [19,22].

One of the authors (T.K.) reported imidazolate-bridged copper(II) complexes $[Cu(\beta\text{-diketonato})(\mu\text{-im})]_x$ (Him stands for imidazole) [23], but their crystal structures have not yet been reported. Generally, there are difficulties in preparing single crystals of polymeric coordination compounds, and also in characterizing compounds as infinite polymers or cyclic oligomers solely from the spectroscopic and elemental analyses. We will report here the crystal structures of $[Cu(dnbm)(\mu\text{-im})]_x$ as two phases, infinite polymer and cyclic tetramer (for structural formula, see below). Preliminary results have been reported in the previous letter [24], and the present report will further discuss the following issue. When the crystal structure analysis is unsuccessful owing to the poor crystallinity, their magnetic measurements would help prediction of crystal structures. The magnetic properties of the complexes whose crystal structures were unknown were analyzed according to the model of a polymer- or tetramer-based spin system.

2. Results

2.1. Preparation

The β-diketones (HL) employed are pentane-2,4-dione (Hacac), heptane-3,5-dione (Hdprm), nonane-4,6-dione (Hdnbm), 2,6-dimethylheptane-3,5-dione (Hdibm), 2,2,6,6-tetramethylheptane-3,5-dione (Hdpm), (1-phenylbutane-1,3-dione (Hbzac) and 1-(2-thienyl)butane-1,3-dione (Htac), and their copper(II) complexes are represented as $[Cu(L)_2]$ (Scheme 1).

Imidazolate-bridged copper(II) complexes $[Cu(L)(\mu\text{-im})]_n$ have been prepared in ethanol [23], and they were efficiently obtained in methanol as well. The reactions of $[Cu(L)_2]$ with two molar equiv. of imidazole gave polymeric complexes $[Cu(L)(\mu\text{-im})]_n$ ($[Cu(acac)(\mu\text{-im})]_n$ (**1p**), $[Cu(dprm)(\mu\text{-im})]_n$ (**2p**), $[Cu(dibm)(\mu\text{-im})]_n$ (**4p**) and $[Cu(dpm)(\mu\text{-im})]_n$ (**5p**)), and tetranuclear $[Cu(bzac)(\mu\text{-im})]_4$ (**6t**). However, $[Cu(dnbm)_2]$ gave tetranuclear $[Cu(dnbm)(\mu\text{-im})]_4$ (**3t**) instead of polymeric $[Cu(dnbm)(\mu\text{-im})]_n$ (**3p**) under these conditions. Complex $[Cu(dnbm)(\mu\text{-im})]_n$ (**3p**) was obtained by the reaction of $[Cu(dnbm)_2]$ with two molar equiv. of imidazole in ethanol. Complex $[Cu(tac)(\mu\text{-im})]_4$ (**7t**) prepared

---

* Corresponding authors. Tel.: +81 42 443 5490; fax: +81 42 443 5501 (T. Ishida).
E-mail addresses: ishi@pc.uec.ac.jp (T. Ishida), kogane@crc.uec.ac.jp (T. Kogane).

0277-5387/$ - see front matter © 2008 Elsevier Ltd. All rights reserved.
doi:10.1016/j.poly.2008.12.004

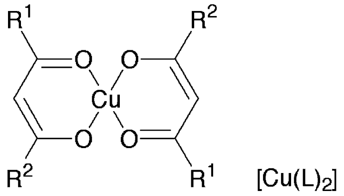

$[Cu(acac)_2]$	$R^1 = R^2 = CH_3$
$[Cu(dprm)_2]$	$R^1 = R^2 = C_2H_5$
$[Cu(dnbm)_2]$	$R^1 = R^2 = n\text{-}C_3H_7$
$[Cu(dibm)_2]$	$R^1 = R^2 = i\text{-}C_3H_7$
$[Cu(dpm)_2]$	$R^1 = R^2 = t\text{-}C_4H_9$
$[Cu(bzac)_2]$	$R^1 = CH_3$, $R^2 = C_6H_5$
$[Cu(tac)_2]$	$R^1 = CH_3$, $R^2 = C_4H_3S$ (2-thienyl)

Scheme 1. Abbreviations and formulas of copper(II) β-diketonates.

according to the previous report [23] was used for the magnetic measurements. Here, the notation **p** and **t** denote polymeric and tetranuclear, respectively.

2.2. Molecular structures

Fig. 1 shows the molecular structure of **3p**. The complex consists of a helix, which has a dinuclear crystallographically independent unit $[\{Cu(dnbm)(\mu\text{-im})\}_2]$ as a repeating motif. The intramolecular nearest-neighboring Cu1···Cu2 and Cu2···Cu1* distances are 5.9016(10) and 5.8973(11) Å, respectively. The Cu ions have a CuN_2O_2 coordination environment with two nitrogen atoms from two imidazolates and two oxygen atoms from a dnbm ligand. Selected geometrical parameters are summarized in Table 1. Although the geometry about the copper ions Cu1 and Cu2 is approximately square-planar, the O1–Cu1–N1, O2–Cu1–N4$^\#$, O3–Cu2–N3, and O4–Cu2–N2 bond angles are considerably smaller than ideal square-planar angle of 180°, being bent toward opposite directions to form a saddle structure. Namely, the coordination around the copper ions is considerably distorted from square-planar toward tetrahedral (d-SP). The Cu1 ion is located slightly above the mean basal O1–O2–N1–N4$^\#$ plane by 0.018(3) Å, and the Cu2 ion above the mean basal O3–O4–N2–N3 plane by 0.053(3) Å.

There are eight copper ions in a pitch along a crystallographic 4_2 screw axis in **3p**, contrary to the expectation from the cis configuration of the N–Cu–N coordination, which seems suitable for a fourfold axis involving four copper ions. It may be related to the d-SP structures at Cu1 and Cu2. The Cu1···Cu2···Cu1* angle (134.66(2)°) is considerably larger than, while the Cu2···Cu1*···Cu2* angle (89.64(2)°) is close to, the ideal right angle. The alternating irregular angles are responsible for the formation of a Cu_8-based chain and not a Cu_4-based helix or a tetrameric macrocycle.

Fig. 2 shows the molecular structure of **4p**. A dinuclear unit is crystallographically independent. A zig-zag chain structure is formed in a space group *C*2/*c*, which contains four copper units in a pitch. As the N–Cu–O angles of 150.37(15)–173.13(15)° indicate, Cu1 has an almost square planer structure (n-SP), while Cu2 has a d-SP one. The dislocations from the mean N_2O_2 planes are small (0.053(12) and 0.031(2) Å, respectively), owing to the saddle structures.

The Cu···Cu distances (5.8865(7) and 5.9239(7) Å) of **4p** are comparable with those of **3p**. The nearest-neighboring Cu···Cu···Cu angles are 102.925(10)° and 132.817(11)°, being suitable for such a zig-zag chain and quite different from that of **3p**. The steric bulkiness of peripheral substituents (*n*-propyl *versus* isopropyl) may affect the molecular packing in the crystal. Basically, the Cu–N and Cu–O distances as well as the N–Cu–N and O–Cu–O angles of **4p** are in typical ranges and just comparable to those of **3p**. Since the Cu–N bonds can rotate in solution, the geometry seems to be fixed in a suitable packing motif on crystallization. Thus, in comparison between **3p** and **4p**, the mutual geometry between neighboring units is different, which is caused by torsion around the Cu–N bonds.

We found that $[Cu(dnbm)(\mu\text{-im})]$ has two phases, **3p** and **3t**. As Fig. 3 shows the molecular structure of **3t**, four Cu ions construct a rectangle arrangement affording a [2 × 2]-molecular grid. A half of the molecule of **3t** is crystallographically independent owing to centrosymmetry in a space group $P\bar{1}$. The intramolecular Cu1···Cu2 and Cu1···Cu2† distances are 5.8694(7) and 5.8933(10) Å, respectively. The Cu2†···Cu1···Cu2 and Cu1···Cu2···Cu1† angles are 89.951(12)° and 90.049(12)°, respectively.

As for the CuN_2O_2 coordination environments in **3t**, the O3–Cu2–N3† and O4–Cu2–N2 are much smaller than the angle of 180°, and, giving saddle-type distortion. Such an out-of-plane deformation has also been reported in the imidazolate-bridged Cu_4 macrocyle [8]. The coordination around the Cu1 ion is n-SP, while Cu2 is d-SP. This finding seems to be similar to that of the bisimidazolato copper(II) compound possessing a d-SP/n-SP-mixed tetranuclear framework. [26]. The dislocations of Cu1 and Cu2 ions are small (0.049(3) and 0.082(3) Å, respectively) from the mean basal N_2O_2 planes, owing to the saddle structures. As the side view (Fig. 3b) shows, the two basal planes are slightly canted with each other by 7.7(1)°.

Fig. 4 shows the molecular structure of **6t**. The refinement was unsatisfactory because **6t** gave only tiny crystals. Large standard deviations remained and thermal displacement factors were somewhat unrealistic for several carbon atoms. However, the *R* factors were decreased to be relatively small (ca. 0.06), and we can safely conclude that **6t** has a tetranuclear macrocyclic structure, or a molecular [2 × 2] grid, in a space group $P\bar{1}$. A dinuclear unit is crystallographically independent. The nearest-neighboring Cu···Cu···Cu angles are nearly 92° and 88°. The molecular structure of **6t** is almost identical to that of **3t** except for the peripheral substituents, and furthermore the molecular packings are also similar to each other in the comparable crystal lattices.

2.3. Magnetic properties

We measured magnetic susceptibilities (χ_{mol}) of polycrystalline specimens of the present compounds on a SQUID magnetometer. The X-ray diffraction study revealed the crystal structures of **3p**, **4p**, **3t**, and **6t**, and we will check the consistency between the structure and magnetic properties. Fig. 5a and 5b show the χ_{mol} versus *T* plots for polymeric **3p** and **4p**, respectively, on the basis of a copper(II) ion.

The χ_{mol} value of **3p** was increased on cooling from 300 K, reached a broad maximum around 60 K, and gradually decreased. This behavior clearly indicates the presence of dominant antiferromagnetic coupling. An extrapolation of the χ_{mol} curvature to 0 K seems to give a non-zero χ_m intercept. Usually such behavior is related with the infinite Heisenberg $S = 1/2$ antiferromagnetic chain, as originally predicted by Bonner and Fisher [27], and so far confirmed by many experiments [28]. Cyclic $S = 1/2$ antiferromagnetic clusters having even number of the spin sources would show null χ_{mol} at $T \to 0$ K. Thus, the non-zero χ_{mol} at $T \to 0$ K is regarded as a fingerprint of infinite chain structures. On further cooling, the χ_{mol} value of **3p** was further decreased with a turning point around 10 K. The origin of this anomaly is not clear at present, but might be explained in terms of a spin-Peierls transition [29]. Namely, a strong singlet–dimer formation takes place to reduce drastically the magnetic susceptibility. To estimate the exchange coupling within a chain, we used the data above 15 K. Assuming the

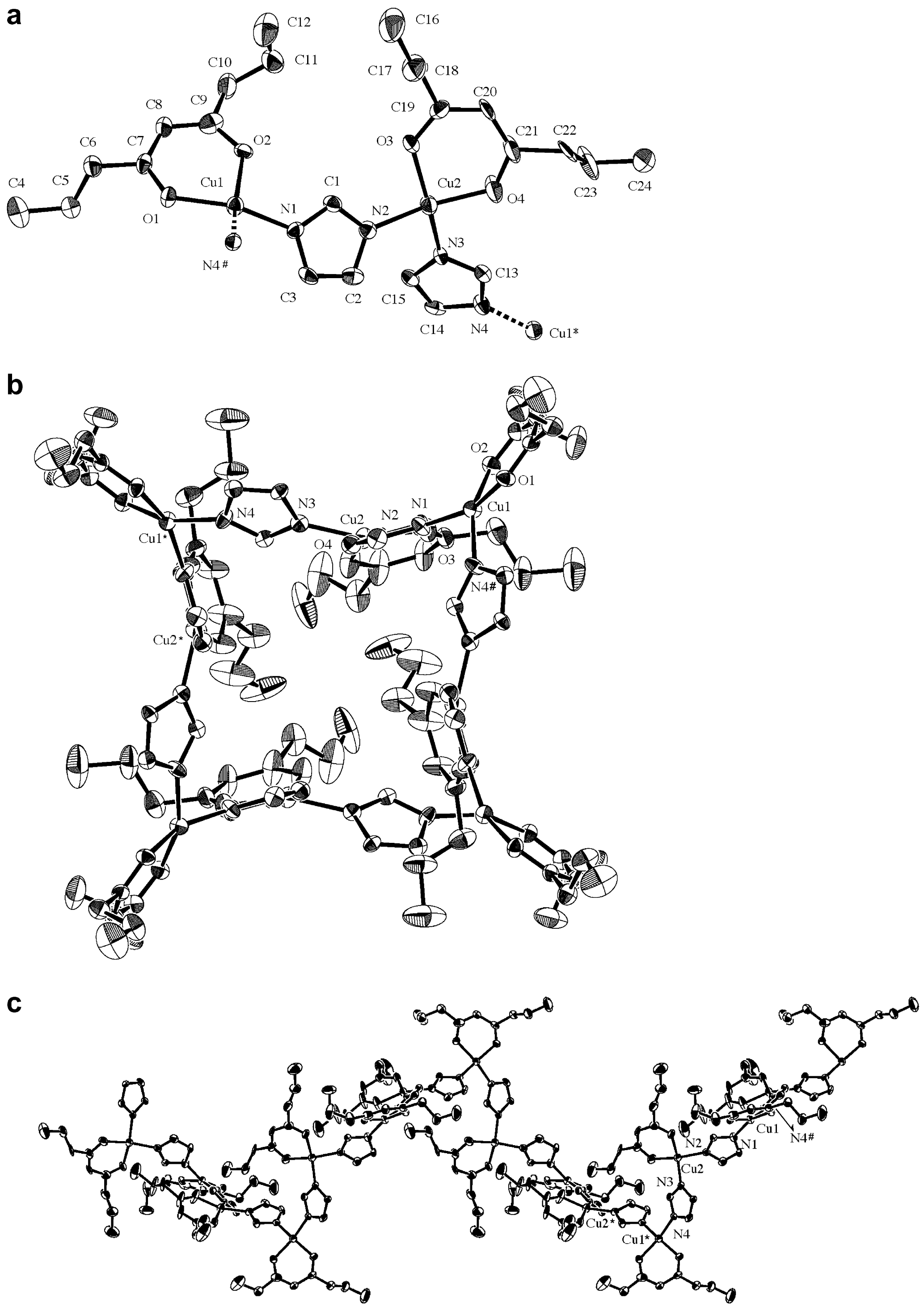

Fig. 1. X-ray crystal structure of [Cu(dnbm)(μ-im)]$_n$ (**3p**). (a) Crystallographically independent unit. Only a major conformation is shown for the C23–C24 portion. Thermal ellipsoids are drawn at the 50% probability level. Hydrogen atoms are omitted. (b) Top and (c) side views of a chain. Eight repeating units are drawn. Symmetry operation codes of $*$ and # are $-y$, $-1/2+x$, $-1/2+z$ and $1/2+y$, $-x$, $1/2+z$, respectively.

equally-spaced $S = 1/2$ magnetic chain and the Heisenberg spin Hamiltonian as $H = -\Sigma 2JS_i \cdot S_{i+1}$, we applied the following expression [27] with $x = |J|/k_\mathrm{B}T$:

$$\chi_\mathrm{mol} = \frac{N_\mathrm{A}\mu_\mathrm{B}^2 g^2}{k_\mathrm{B}T}\,\frac{0.25 + 0.14995x + 0.30094x^2}{1.0 + 1.9862x + 0.68854x^2 + 6.0626x^3}. \tag{1}$$

The best fit gave −89.8(7) K with $g = 2.04(2)$ for **3p**. According to the Bonner–Fisher analysis, T_max at which χ_mol shows a rounded maximum is simply related with J as expressed by Eq. (2) [27]. The χ_m peak position around 60 K for **3p** agrees well with the calculated J value:

$$k_\mathrm{B}T_\mathrm{max}/\,|\,J\,| = \text{ca. } 1.28. \tag{2}$$

Similarly, **4p** exhibited a Bonner–Fisher-type behavior (Fig. 5b). However, in sharp contrast to the case of **3p**, the χ_mol value of **4p** turned to increase again below 10 K, suggesting a slight contamination with Curie impurity. We analyzed the experimental data using the Bonner–Fisher model plus a Curie contribution (Eq. (3)).

Table 1
Selected bond lengths (Å) and angles (°).

Compounds	3p	4p	3t
Cu1–O1	1.918(3)	1.938(3)	1.913(3)
Cu1–O2	1.932(4)	1.935(3)	1.929(4)
Cu1–N1	1.954(5)	1.958(3)	1.935(4)
Cu1–N4	1.954(5)[a]	1.977(3)[b]	1.932(5)[c]
Cu2–O3	1.923(4)	1.950(3)	1.919(4)
Cu2–O4	1.920(4)	1.926(3)	1.918(3)
Cu2–N2	1.981(5)	1.941(3)	1.957(3)
Cu2–N3	1.944(5)	1.954(3)	1.967(4)
O1–Cu1–N1	158.46(19)	173.13(15)	154.9(2)
O2–Cu1–N4	156.73(18)[a]	167.59(16)[b]	152.2(2)[c]
O3–Cu2–N3	159.08(19)	150.37(15)	162.6(2)
O4–Cu2–N2	161.3(2)	152.82(15)	171.5(2)

[a] N4 is a symmetry-related equivalence with $-y$, $-1/2+x$, $-1/2+z$.
[b] N4 is a symmetry-related equivalence with $1/2-x$, $-1/2+y$, $3/2-z$.
[c] N4 is a symmetry-related equivalence with $1-x$, $2-y$, $-z$.

$$\chi_{\mathrm{mol}} = \frac{N_{\mathrm{A}}\mu_{\mathrm{B}}^2 g^2}{k_{\mathrm{B}}T}\,\frac{0.25+0.14995x+0.30094x^2}{1.0+1.9862x+0.68854x^2+6.062x^3}+\frac{C_{\mathrm{imp}}}{T}. \qquad (3)$$

The best fit gave $2J/k_B = -93.1(6)$ K with $g = 2.129(5)$ and $C_{\mathrm{imp}} = 0.00695(4)$ cm^3 mol^{-1} for **4p**. The obtained J is very close to that of **3p**, despite of the different helix motives.

Although the crystal structures of **1p**, **2p**, and **5p** are unknown, we measured their magnetic susceptibility to predict the crystal structures. Fig. 6 shows the results of them. They showed a broad maximum and non-zero χ_{mol} at $T \to 0$ K. This behavior strongly suggests that they are antiferromagnetically correlated infinite chains, just like **3p** and **4p**. There also were Curie tails. The Bonner–Fisher model (i.e., Eq. (3)) was applied, giving $2J/k_B = -96(2)$ K, $g = 2.01(4)$, and $C_{\mathrm{imp}} = 0.00725(9)$ cm^3 K mol^{-1} for **1p**, $2J/k_B = -96.9(3)$ K, $g = 2.09(2)$, and $C_{\mathrm{imp}} = 0.0086(2)$ cm^3 K mol^{-1} for **2p**, and $2J/k_B = -85(1)$ K, $g = 2.13(2)$, and $C_{\mathrm{imp}} = 0.00232(8)$ cm^3 K mol^{-1} for **5p**. The calculated curves well reproduced the experimental data (solid lines in Fig. 6). Thus, we assume that they would be chains.

The content of the Curie impurity varied from 0.6% to 2% depending on the specimens investigated here, but the coupling parameters are close to each other (from −85 to −97 K for **1p**–**5p**). This finding supports the assumption that the structurally common bridges Cu–N(eq)–N(eq)–Cu afford comparable magnitudes of couplings. They largely depend on the coordination sites, equatorial and axial, where the nitrogen atoms are coordinated [30].

The χ_{mol} versus T pots of tetrameric **3t** and **6t** (Fig. 7) exhibited a distinctly different feature from those of **3p** and **4p**. Namely, zero χ_{mol} values are suggested at $T \to 0$ K. As for **3t**, the χ_{mol} value increased on lowering temperature and reached a maximum around 55 K. After that the χ_{mol} value turned to decrease somewhat steeply toward $\chi_{\mathrm{mol}} = 0$ cm^3 mol^{-1}. A Curie impurity was included, as indicated with a sharp upturn at the lowest temperature region.

A square model involving four $S = 1/2$ spins leads to the Heisenberg spin Hamiltonian as $H = -2J(S_1 \cdot S_2 + S_2 \cdot S_3 + S_3 \cdot S_4 + S_4 \cdot S_1)$. The molar magnetic susceptibility can be written as Eq. (4) [6,7,10] by applying Kambe's vector coupling method [31] and the van Vleck equation:

$$\chi_{\mathrm{mol}} = \frac{N_{\mathrm{A}}\mu_{\mathrm{B}}^2 g^2}{k_{\mathrm{B}}T}\,\frac{2+5\exp(2J/k_{\mathrm{B}})+\exp(-2J/k_{\mathrm{B}})}{7+5\exp(2J/k_{\mathrm{B}})+3\exp(-2J/k_{\mathrm{B}})+\exp(-4J/k_{\mathrm{B}})} + \frac{C_{\mathrm{imp}}}{T}. \qquad (4)$$

A Curie impurity term was added. The experimental data of **3t** were fitted to Eq. (4) to give $2J/k_B = -81.0(2)$ K, $g = 2.061(2)$, and

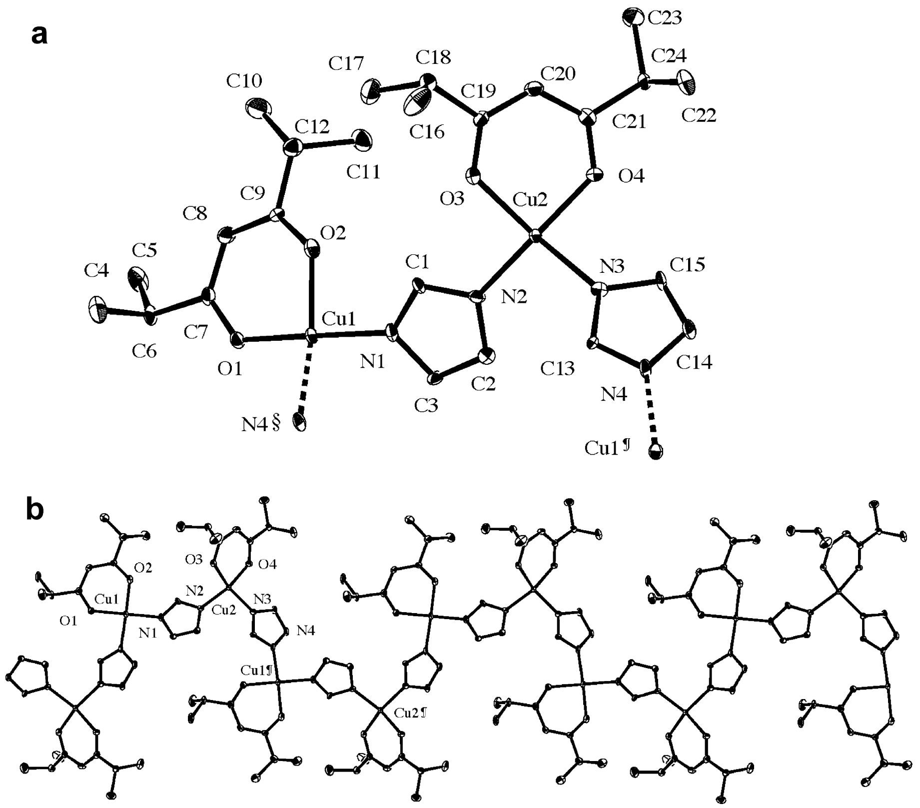

Fig. 2. X-ray crystal structure of [Cu(dibm)(μ-im)]$_n$ (**4p**). (a) Crystallographically independent unit. Thermal ellipsoids are drawn at the 50% probability level. Hydrogen atoms are omitted. (b) Side views of a chain. Six repeating units are drawn. Symmetry operation codes of § and ¶ are $1/2-x$, $-1/2+y$, $3/2-z$, and $1/2-x$, $1/2+y$, $3/2-z$, respectively.

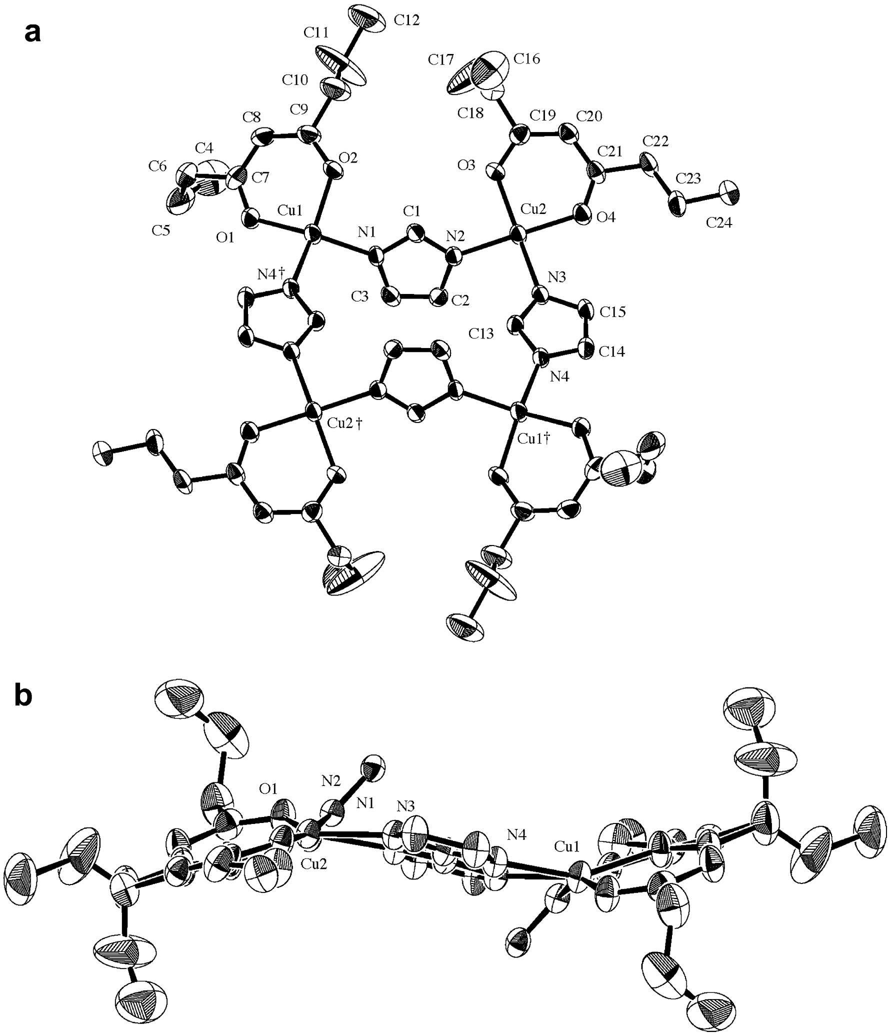

Fig. 3. X-ray crystal structure of $[Cu(dnbm)(\mu\text{-}im)]_4$ (**3t**). (a) Top and (b) side views. Thermal ellipsoids are drawn at the 30% probability level. Hydrogen atoms are omitted. Symmetry operation code of † is $1-x$, $2-y$, $-z$.

$C_{imp} = 0.0203(2)\ cm^3\ K\ mol^{-1}$. The dotted line in Fig. 7a implies the first term in Eq. (3) after the subtraction of the Curie term. This line approaches to $0\ cm^3\ mol^{-1}$ at $T \rightarrow 0$ K.

The data of **6t** were similarly analyzed (Fig. 7b). The data on **6t** were fitted to Eq. (4) and the parameters were optimized as: $2J/k_B = -78(1)$ K, $g = 2.13(2)$, and $C_{imp} = 0.00662(8)\ cm^3\ K\ mol^{-1}$. The J value is very close to that of **3t**.

The crystal structure of **7t** is unknown, but we measured its magnetic susceptibility (Fig. 7b). The data on **7t** were also well fitted to Eq. (4) rather than Eq. (3). The molecular structure was suggested to be a square tetramer. The parameters were optimized as: $2J/k_B = -85.0(8)$ K, $g = 2.27(1)$, and $C_{imp} = 0.00230(6)\ cm^3\ K\ mol^{-1}$. The calculated curves well reproduced the experimental data. Thus, we predict that **7t** would consist of a cyclic tetramer.

3. Discussion

3.1. Synthesis

Complexation reactions of $[Cu(L)_2]$ with imidazole are very sensitive to the nature of the β-diketonato ligand as well as to the reaction conditions, sometimes giving different products depending upon the solvent used. For convenience, $[Cu(L)_2]$ can be classified into $[Cu(L^1)_2]$, $[Cu(L^2)_2]$, and $[Cu(L^3)_2]$ (HL^1, HL^2, and HL^3 stand for aliphatic β-diketones, aroyl- or hetaroylacetones and fluorinated β-diketones, respectively).

The reactions of $[Cu(L^1)_2]$ and $[Cu(L^2)_2]$ with two molar equiv. of imidazole in methanol or ethanol gave polymeric and tetranuclear complexes ($[Cu(L^1)(\mu\text{-}im)]_n$ and $[Cu(L^2)(\mu\text{-}im)]_4$), respectively. The $[Cu(dnbm)_2]$ case is exceptional. A mixture of $[Cu(dnbm)_2]$ with two molar equiv. of imidazole gave **3t** under the same conditions. On the other hand, when a mixture solution was concentrated gradually on heating, yielding **3p** (see Section 5).

Complexation reactions of $[Cu(L)_2]$ with pyrazole gave different products. The complexes $[Cu(L^1)_2]$ afforded di- or tetranuclear complexes, while $[Cu(L^2)_2]$ afforded pyrazolate-bridged complexes, 1:1 and/or 1:2 adducts [32]. Furthermore, $[Cu(L^1)_2]$ afforded different products depending upon the solvents used. By successive addition of imidazole, $[Cu(acac)_2]$ gave no isolable imidazolate complex in chloroform [25], while gave **1p** instead of the imidazolate complex in ethanol or methanol [23]. It has been reported that $[Cu(L^3)_2]$ such as $[Cu(hfac)_2]$ (Hhfac stands for 1,1,1,5,5,5-hexafluoropentane-2,4-dione) afforded 1:1 and/or 1:2 adducts in chloroform because of their stronger coordination ability [25].

3.2. Crystal structures

Chaudhuri et al. prepared cyclic tri- and tetranuclear copper(II) complexes [5,6], where non-substituted imidazolate was utilized

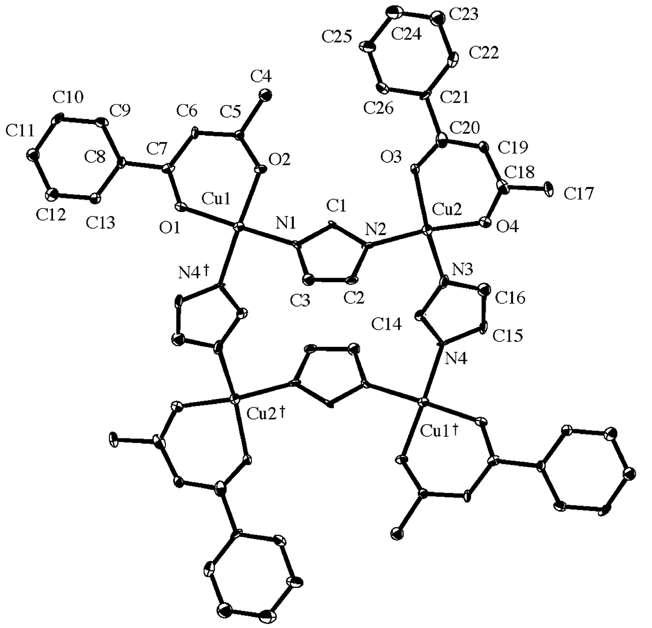

Fig. 4. X-ray crystal structure of $[Cu(bzac)(\mu\text{-}im)]_4$ (**6t**). Thermal ellipsoids are drawn at the 50% probability level. Hydrogen atoms are omitted. Symmetry operation code of † is $2 - x$, $1 - y$, $-z$.

as a bridge; namely, $[Cu_3(tacn)_3(\mu\text{-}im)_3](ClO_4)_3$ and $[Cu_4(tacn)_4(\mu\text{-}im)_4](ClO_4)_4 \cdot 2H_2O$ (tacn = 1,4,7-triazacyclononane). The capping ligands are tridentate and neutral. Consequently, the copper ions were square-pyramidal. Counter ions (ClO_4^-) did not work as ligands. On the other hand, the present compounds have monoanionic β-diketonate chelates as a cap. All of the copper ions are tetra-coordinated (actually n-SP and d-SP). There is no counter anion in the crystal lattice. However, the tetranuclear skelton $[Cu_4(\mu\text{-}im)_4]$ of **3t** is similar to that of $[Cu_4(tacn)_4(\mu\text{-}im)_4](ClO_4)_4 \cdot 2H_2O$ [6] as well as other known tetramers [7–10].

In the present study, the capping ligands are simple β-diketonates, which occupy two equatorial sites in a cis manner. Accordingly, the imidazolate N atoms are coordinate at the rest position in a cis manner. The N(im)–Cu–N(im) angles close to 90° favors tetranuclear macrocycles. Though several imidazolate-based preorganized ligands have been utilized for development of [2 × 2] grids [6–10], the combination of commercially available copper(II) diketonates and the unsubstituted imidazolate ion is also versatile for this purpose.

3.3. Magnetic properties

The magnetic data of **1p**–**5p** were analyzed by the Bonner–Fisher model as an equally-spaced model. We have to think possible fittings to alternating-chain and rectangle models, because the crystallographic analysis indicates that there are two kinds of exchange couplings. The present analysis brought about averaged values from two independent parameters, J and αJ, where α is alternation parameter. In more precise treatment using the Heisenberg spin Hamiltonian as $H = -\Sigma(2JS2_{2i-1} \cdot S_{2i} + 2\alpha J S_{2i} \cdot S_{2i+1})$, we could adopt an alternating antiferromagnetic chain model [33]. One may imagine the singlet–triplet model [34] in case of the $\alpha = 0$ limit, and accordingly the χ_{mol} value approaches to null at $T \to 0$ K when α is close to zero. On the other hand, the χ_{mol} versus T profile appears just like the Bonner–Fisher curve when α is close to unity. The present results on **1p**–**5p** exhibited the non-zero χ_{mol} at the $T \to 0$ K limit, which guarantees that an approximation as an equally-spaced chain model is valid. Moreover, the possibility of

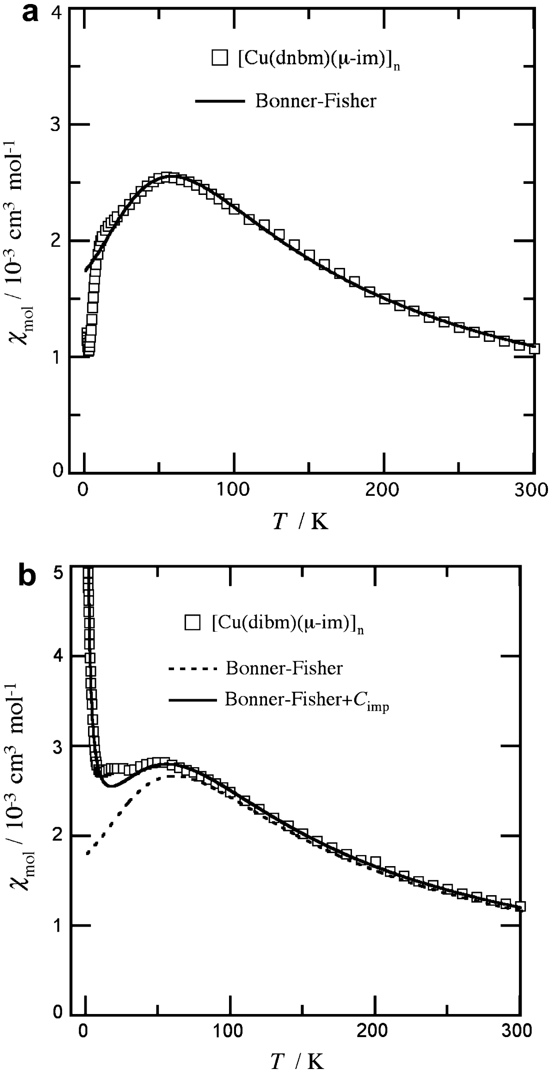

Fig. 5. Temperature dependence of molar magnetic susceptibility (χ_{mol}) for (a) $[Cu(dnbm)(\mu\text{-}im)]_n$ (**3p**) and (b) $[Cu(dibm)(\mu\text{-}im)]_n$ (**4p**). The solid and dotted lines represent the best fit curves. See the text for the equations and parameters.

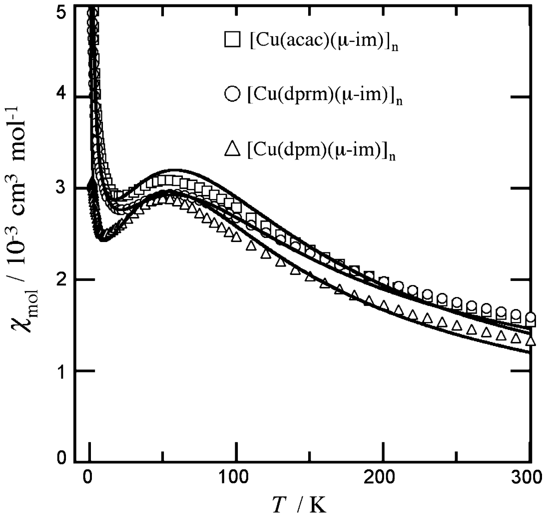

Fig. 6. Temperature dependence of molar magnetic susceptibility (χ_{mol}) for $[Cu(acac)(\mu\text{-}im)]_n$ (**1p**), $[Cu(dprm)(\mu\text{-}im)]_n$ (**2p**), and $[Cu(dpm)(\mu\text{-}im)]_n$ (**5p**). The solid lines represent the best fit curves. See the text for the equations and parameters.

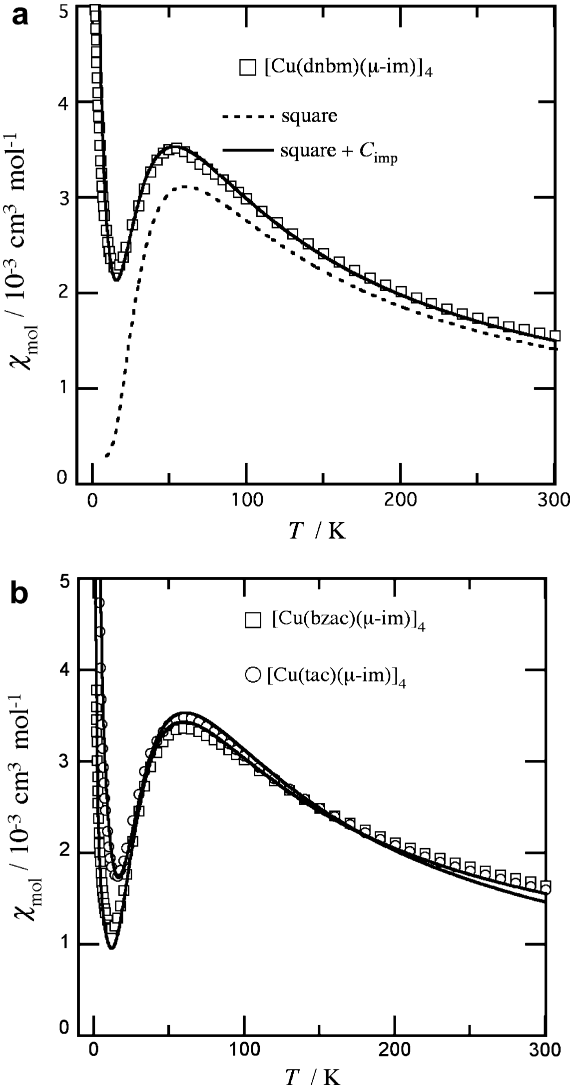

Fig. 7. Temperature dependence of χ_{mol} for (a) [Cu(dnbm)(μ-im)]$_4$ (**3t**) and (b) [Cu(bzac)(μ-im)]$_4$ (**6t**) and [Cu(tac)(μ-im)]$_4$ (**7t**). The solid and dotted lines represent the best fit curves. See the text for the equations and parameters.

the cyclic structures such as a tetramer is completely discarded. Compounds **1p**, **2p**, and **5p** consist of chains as well as **3p** and **4p**. The reports on imidazolate-bridged copper(II) chains are rare [17,18], in which the copper ions were weekly bonded with ligands in an axial manner. To our knowledge, the present work is the first characterization of one-dimensional imidazolate-bridged copper(II) chains showing appreciable antiferromagnetic couplings.

The magnetic data of **3t**, **6t**, and **7t** were analyzed by the square model as an equally-spaced model. Similarly, possibility of rectangle models deserves discussion, because the crystallographic analysis indicates that there are two crystallographic independent copper ions in a tetramer. We actually tried to fit the data of **7t** as well as **3t** and **6t** to the alternating antiferromagnetic chain model [32] and the rectangle model [7]. We eventually found that the latter analysis more likely from the better fit. Furthermore, we also found that the analysis based on the equal spacing satisfactorily reproduced the experimental results.

The structurally common bridges Cu–N$_{im}$(eq)–N$_{im}$(eq)–Cu afford comparable magnitudes of couplings. The 2J values were observed between −78 and −97 K for both the chains and cycles investigated here, and accordingly the α value should be 0.80 at the most. Hence, though an alternating parameter α should be introduced, α was found to be close to unity.

The exchange parameters for the present compounds fell in a typical range of superexchange couplings between copper(II) ions across imidazolates [5–10]. The mechanism of the superexchange coupling was previously discussed by Kolks et al. [7] and Chaudhuri et al. [6]. The σ-pathway across the nitrogen lone-pairs has been pointed out, like other diazaaromatic-bridged systems [35]. The present exchange couplings are much larger than that of imidazolate-bridged copper(II) chains having the *N*-equatorial–*N*-axial bridging motif (for example, $2J/k_B = -5.2$ K [18]).

4. Concluding remarks

The magnetic properties of **1p**–**5p**, **3t**, **6t**, and **7t** were found to be devided into two categories: the Bonner–Fisher model was plausibly applied to polymeric [Cu(L)(μ-im)]$_n$ for the best fit, while a square model to tetrameric [Cu(L)(μ-im)]$_4$. We could not determine the crystal structures of **1p**, **2p**, **5p**, and **7t** at present. It is difficult to characterize compounds as infinite polymers or cyclic oligomers solely from the spectroscopic and elemental analyses. The polymeric and tetranuclear structures could be clearly distinguished from each other by fitting the magnetic data to theoretical curves.

We utilized a simple imidazolate anion for linking several copper(II) diketonates without preorganization of the ligands. It should be noted that the combination of simple copper(II) diketonates and imidazolate ion is versatile for supramolecular chemistry.

5. Experimental

5.1. Materials

Bis(β-diketonato)copper(II) complexes employed were [Cu(acac)$_2$], [Cu(dprm)$_2$], [Cu(dnbm)$_2$], [Cu(dibm)$_2$], [Cu(dpm)$_2$] and [Cu(bzac)$_2$]. They were prepared by the reported method [23]. Imidazole (Tokyo Chemical Industry Co.) was recrystallized from light petroleum (b.p. range 30–70 °C).

The imidazolate-bridged complexes **1p**–**5p** and **6t** are previously characterized except for melting points. However, these complexes and **3t** were prepared for X-ray diffraction study and magnetic measurements according to the following method. Complex **7t** prepared by the previous report [23] was applied for magnetic measurements.

[Cu(acac)(μ-im)]$_n$ (**1p**). The complex [Cu(acac)$_2$] (103.2 mg, 0.39 mmol) was dissolved in methanol (20 ml) with two molar equiv. of imidazole (53.3 mg, 0.78 mmol). The solution was refluxed for 2 h. After standing for a few days, a violet precipitate was formed. The product was filtered, washed with a small amount of methanol, and dried *in vacuo*. The yield was 33.5 mg (37%). Mp. 182–185 °C.

[Cu(dprm)(μ-im)]$_n$ (**2p**). This complex was prepared according to a similar method to that described for **1p**. The yield was 39%. Mp. 183–186 °C.

[Cu(dnbm)(μ-im)]$_n$ (**3p**). The complex [Cu(dnbm)$_2$] (74.8 mg, 0.20 mmol) was dissolved in ethanol (15 ml) with two molar equiv. of imidazole (27.3 mg, 0.40 mmol). The solution was refluxed for 2 h and the solvent was concentrated gradually on heating. Black fine needles were formed during the concentration. They were filtered, washed with a small amount of ethanol, and dried *in vacuo*, giving 17.3 mg of **3p** (30%). Mp. 153–156 °C.

[Cu(dnbm)(μ-im)]$_4$ (**3t**). The complex [Cu(dnbm)$_2$] (74.8 mg, 0.20 mmol) was dissolved in ethanol (15 ml) with two molar equiv. of imidazole (27.3 mg, 0.40 mmol). The solution was stirred at

Table 2
Selected crystallographic data for **3p**, **4p**, **3t**, and **6t**.

Compounds	**3p**	**4p**	**3t**	**6t**
Formula	$C_{12}H_{18}CuN_2O_2$	$C_{12}H_{18}CuN_2O_2$	$C_{48}H_{72}Cu_4N_8O_8$	$C_{52}H_{48}Cu_4N_8O_8$
Formula weight	285.83	285.83	1143.32	1167.18
Habit	black block	blue platelet	blue prism	blue prism
Dimension (mm^3)	0.36 × 0.18 × 0.09	0.2 × 0.2 × 0.2	0.51 × 0.4 × 0.24	0.08 × 0.05 × 0.01
T (K)	97	90	296	90
Crystal system	tetragonal	monoclinic	triclinic	triclinic
Space group	$P4_2/n$	$C2/c$	$P\bar{1}$	$P\bar{1}$
a (Å)	21.047(15)	28.03(4)	8.396(6)	8.168(18)
b (Å)	21.047(15)	16.91(2)	12.616(6)	11.39(3)
c (Å)	12.334(11)	11.125(18)	13.738(8)	13.16(3)
α (°)	90	90	93.78(4)	95.23(7)
β (°)	90	95.03(6)	99.89(5)	91.78(6)
γ (°)	90	90	106.49(5)	103.72(7)
V (Å^3)	5764(7)	5254(13)	1364.3(14)	1183(5)
Z	16	16	1	1
D_{calc} (g cm^{-3})	1.390	1.445	1.391	1.639
Unique data	5764	6012	5987	5353
μ (Mo Kα) (mm^{-1})	1.591	1.655	1.593	1.840
R (F)[a] ($I > 2\sigma(I)$)	0.0566	0.0546	0.0580	0.0569
$R_w(F^2)$[b] (all data)	0.0588	0.0978	0.0737	0.0806

[a] $R = \Sigma||F_o| - |F_c||/\Sigma|F_o|$.

[b] $R_w = [\sum w(F_0^2 - F_o^2)^2 / \sum w(F_o^2)]^{1/2}$.

room temperature for 2 h, and allowed to stand at room temperature for 10 days. The resultant bluish black blocks were filtered, washed with a small amount of ethanol, and dried *in vacuo*. The yield was 10.3 mg (18%). Mp. 113–114 °C.

[Cu(dibm)(μ-im)]$_n$ (**4p**). The complex [Cu(dibm)$_2$] (50.8 mg, 0.14 mmol) was dissolved in methanol (10 ml) with two molar equiv. of imidazole (18.4 mg, 0.27 mmol). The solution was refluxed for 2 h. After standing for a few days, dark blue needles were formed. They were filtered, washed with a small amount of methanol, and dried *in vacuo*. The yield was 16.2 mg (40%). Mp. 183–185 °C.

[Cu(dpm)(μ-im)]$_n$ (**5p**). This complex was prepared by a similar method to that described for complex **1p**. The yield was 85%. Mp. >195 °C.

[Cu(bzac)(μ-im)]$_4$ (**6t**). The complex [Cu(bzac)$_2$] (100.2 mg, 0.26 mmol) was dissolved in methanol (25 ml) with two molar equiv. of imidazole (35.3 mg, 0.52 mmol). The solution was refluxed for 2 h. After standing for a few days, dark green crystals were formed. They were filtered, washed with a small amount of methanol and dried *in vacuo*. The yield was 35.1 mg (46%). Mp. 185–187 °C.

5.2. X-ray crystallographic analysis

X-Ray diffraction data of **3p, 4p, 3t**, and **6t** were collected on a Rigaku R-axis RAPID diffractometer or a Rigaku Saturn-70 CCD diffractometer with graphite monochromated MoKα radiation ($\lambda = 0.71069$ Å). The structures were directly solved by a heavy-atom method and expanded using Fourier techniques in the CRYSTALSTRUCTURE 3.8.2 program package [36]. Numerical absorption correction was used. All of the hydrogen atoms were located at calculated positions and the parameters were refined as "riding". The thermal displacement parameters of non-hydrogen atoms were refined anisotropically. Full-matrix least-squares methods were applied using all of the unique reflection data. Selected crystallographic data are listed in Table 2. Preliminary crystallographic analysis on **6t** was also performed.

5.3. Magnetic measurements

Magnetic properties of polycrystalline specimens of **1p–5p, 3t, 6t,** and **7t** were measured at 5000 Oe in a temperature range down to 1.8 K on a Quantum Design MPMS SQUID magnetometer. The magnetic responses were corrected with diamagnetic blank data of the sample holder measured separately. The diamagnetic contribution of the sample itself was estimated from Pascal's constants.

Acknowledgements

This work was supported by Grants-in-Aid for Scientific Research (Nos. 15073101, 16550121, and 19550135) from the Ministry of Education, Culture, Sports, Science and Technology, Japan.

Appendix A. Supplementary data

CCDC 702612, 702613, 702869, and 702870 contain the supplementary crystallographic data for **3p**, **3t**, **4p**, and **6t**, respectively. These data can be obtained free of charge via http://www.ccdc.cam.ac.uk/conts/retrieving.html, or from the Cambridge Crystallographic Data Centre, 12 Union Road, Cambridge CB2 1EZ, UK; fax: (+44) 1223-336-033; or e-mail: deposit@ccdc.cam.ac.uk. Supplementary data associated with this article can be found, in the online version, at doi:10.1016/j.poly.2008.12.004.

References

[1] O. Kahn, Molecular Magnetism, VCH, New York, 1993.
[2] M. Eddaoudi, D.B. Moler, H. Li, B. Chen, T.M. Reineke, M. O'Keefe, O.M. Yaghi, Acc. Chem. Res. 34 (2001) 319.
[3] J.-M. Lehn, Supramolecular Chemistry: Concepts and Perspective, VCH, Weinheim, 1995.
[4] A. Messerschmidt, R. Huber, Eur. J. Biochem. 187 (1990) 341.
[5] P. Chaudhuri, I. Karpenstein, M. Winter, C. Butzlaff, E. Bill, A.X. Trautwein, U. Florke, H.J. Haupt, J. Chem. Soc., Chem. Commun. (1992) 321.
[6] P. Chaudhuri, I. Karpenstein, M. Winter, M. Lengen, C. Butzlaff, E. Bill, A.X. Trautwein, U. Flörke, H.-J. Haupt, Inorg. Chem. 32 (1993) 888.
[7] G. Kolks, S.J. Lippard, J.V. Waszezak, H.R. Lilienthal, J. Am. Chem. Soc. 104 (1982) 717.
[8] S. Mukherjee, T. Weyhermüller, E. Bill, P. Chaudhuri, Eur. J. Inorg. Chem. (2001) 4209.
[9] W.A. Alves, G. Cerchiaro, A. Paduan-Filho, D.M. Tomazela, M.N. Eberlin, A.M.D.C. Ferreira, Inorg. Chim. Acta 358 (2005) 3581.
[10] T. Higa, M. Moriya, Y. Shimazaki, T. Yajima, F. Tani, S. Karasawa, M. Nakano, Y. Naruta, O. Yamauchi, Inorg. Chim. Acta 360 (2007) 3304.
[11] C.A. Koch, C.A. Reed, G.A. Brewer, N.P. Rath, W.R. Scheidt, G. Gupta, G. Lang, J. Am. Chem. Soc. 111 (1989) 7645.
[12] (a) E. Colacio, M. Ghazi, R. Klevekas, M. Klinga, F. Lloret, J.M. Moreno, Inorg. Chem. 39 (2000) 2770;

(b) E. Colacio, J.M. Dominguez-Vera, M. Ghazi, R. Liveskas, M. Klinga, J.M. Moreno, Inorg. Chem. 37 (1998) 3040.

[13] N. Matsumoto, K. Inoue, M. Ohba, H. Okawa, S. Kida, Bull. Chem. Soc. Jpn. 65 (1992) 2283.

[14] J.M. Dominguez-Vera, N. Galvez, E. Colacio, R. Cuesta, J.-P. Costes, J.-P. Laurent, J. Chem. Soc., Dalton Trans. (1996) 861.

[15] R. Boca, M. Hvastijova, J. Kozisek, M. Valko, H. Ehrenberg, H. Fuess, W. Haase, I. Svoboda, R. Werner, Inorg. Chem. Commun. 8 (2005) 548.

[16] Y.F. Song, C. Massera, M. Quesada, I.A. Koval, Patrick Gamez, A.M.M. Lanfredi, J. Reedijk, Eur. J. Inorg. Chem. (2004) 4566.

[17] S.H. Rahaman, H. Chowdhury, D. Bose, G. Mostafa, H.-K. Fun, B.K. Ghosh, Inorg. Chem. Commun. 8 (2005) 1041.

[18] N. Matsumoto, T. Nozaki, H. Ushio, K. Motoda, M. Ohba, G. Mago, H. Okawa, J. Chem. Soc., Dalton Trans. (1993) 2157.

[19] N. Masciocchi, S. Bruni, E. Cariati, F. Cariati, S. Galli, A. Sironi, Inorg. Chem. 40 (2001) 5897.

[20] N. Masciocchi, G.A. Ardizzoia, G. LaMonica, A. Maspero, S. Galli, A. Sironi, Inorg. Chem. 40 (2001) 6983.

[21] (a) S.J. Retting, A. Storr, D.A. Suumers, R.C. Thompson, J. Trotter, J. Am. Chem. Soc. 119 (1997) 8675;
(b) S.J. Retting, V. Sanchez, A. Storr, R.C. Thompson, J. Trotter, J. Chem. Soc., Dalton Trans. (2000) 3931.

[22] (a) Y.-Q. Tian, C.-X. Cai, X.-M. Ren, C.-Y. Duan, Y. Xu, S. Gao, X.-Z. You, Chem. Eur. J. 9 (2003) 5673;
(b) J.-P. Zhang, X.-M. Chen, Chem. Commun. (2006) 1689.

[23] T. Kogane, R. Hirota, Bull. Chem. Soc. Jpn. 53 (1980) 91.

[24] R. Watanabe, N. Koyama, T. Nogami, T. Ishida, T. Kogane, Chem. Lett. 38 (2009) 30.

[25] J.T. Chen, S.M. Wang, J. Chin. Chem. Soc. 18 (1971) 213.

[26] (a) J. Peisach, P. Aisen, W.E. Blumberg, The Biochemistry of Copper, Academic Press, 1966;
(b) J.A.J. Jarvis, A.F. Wells, Acta Crystallogr. 13 (1960) 1027.

[27] J.C. Bonner, M.E. Fisher, Phys. Rev. A 135 (1964) 640.

[28] (a) R. Feyerherm, S. Abens, D. Günther, T. Ishida, M. Meissner, M. Meschke, T. Nogami, M. Steiner, J. Phys.: Condens. Matter 12 (2000) 8495;
(b) R. Feyerherm, T. Ishida, T. Nogami, M. Seiner, Mol. Cryst. Liq. Cryst. 335 (1999) 947.

[29] (a) J.S. Miller, Extended Linear Chain Compounds, Plenum Press, New York, 1983;
(b) K. Mukai, N. Wada, J.B. Jamali, N. Achiwa, Y. Narumi, K. Kindo, T. Kobayashi, K. Amaya, Chem. Phys. Lett. 257 (1996) 538.

[30] (a) N. Koyama, T. Ishida, T. Nogami, T. Kogane, Polyhedron 27 (2008) 2341;
(b) M. Yasui, Y. Ishikawa, N. Akiyama, T. Ishida, T. Nogami, F. Iwasaki, Acta Crystallogr., Sect. B 57 (2001) 288.

[31] K. Kambe, J. Phys. Soc. Jpn 5 (1950) 48.

[32] T. Kogane, T. Yamamoto, M. Hayashi, R. Hirota, C.A. Horiuchi, Polyhedron 14 (1995) 2475.

[33] (a) W.E. Estes, D.P. Gavel, W.E. Hatfield, D. Hodgson, Inorg. Chem. 17 (1978) 1415;
(b) W.E. Hatfield, J. Appl. Phys. 52 (1981) 1985.

[34] B. Bleaney, K.D. Bowers, Proc. R. Soc. London, Ser. A 214 (1952) 451.

[35] T. Ishida, T. Kawakami, S.-i. Mitsubori, T. Nogami, K. Yamaguchi, H. Iwamura, J. Chem. Soc., Dalton Trans. (2002) 3177.

[36] CRYSTALSTRUCTURE, version 3.8.2, Rigaku/MSC, The Woodlands, TX 77381, 2003–2007, USA.